Journal of Advanced Joining Processes 2 (2020) 100030

Contents lists available at ScienceDirect

Journal of Advanced Joining Processes

journal homepage: www.elsevier.com/locate/jajp

A review: Interlayer joining of nickel base alloys

William Reeks [a,*], Helen Davies [b], Silvia Marchisio [b]

[a] Institute of Structural Materials, Bay Campus, Swansea University, Swansea SA1 8EN, UK
[b] Rolls-Royce plc, P.O. Box 31, Derby DE24 8BJ, UK

ARTICLE INFO

Keywords:
Nickel alloys
Interlayer bonding
Diffusion bonding
Dissimilar joining
Titanium alloys

ABSTRACT

This article provides a comprehensive review of the improvements and results in interlayer bonding of nickel and its alloys to other metal alloys. The development of the interlayer bonding process in joining nickel-based alloys is of high interest to the aerospace and power generation industries, with the idea of on-site repair of turbine components of focus. History of the diffusion bonding process has been summarized, and bonding parameters and methods for various alloy combinations have been outlined. The relationship between hardness and strength, to the intermetallic compounds and porosity present in the bond region has been illustrated. The literature shows the methods for manipulating the volume of these compounds, and subsequent strength. The paper also shows the microstructural changes that occur during interlayer bonding and how these may be manipulated by changing bonding parameters and interlayer composition. Recent and influential papers have been summarized, with the key findings outlined, the type of interlayer and alloy/s being joined have been headlined for ease of navigation, when available, bond strengths and mechanical property values have been highlighted to illustrate bond soundness. This review does not concern traditional fusion welding methods.

Introduction

8% of operating costs for airline operators are for engine maintenance and repair, and so techniques that have the potential to join high-performance alloys using relatively low energies are of strong interest (Aschenbruck et al., 2014). Interlayer bonding has been used to join various alloys used in the aerospace industry with good success (Davies et al., 2019; Stanners et al., 2020; Xiong et al., 2019). Other joining processes such as beam welding or friction welding have been used to join nickel superalloys, though these techniques typically favor thicker components due to the much greater amount of energy involved (Sekhar and Reed, 2002; Preuss et al., 2006). Laser welding of nickel alloys often results in very weak, brittle joints; interlayers have been shown to drastically improve soundness of the bond.

Nickel-based superalloy components typically make up approximately 40% of the modern gas turbine by mass and are typically critical to the operation of the engine. These alloys are known for their impressive mechanical properties at elevated temperatures, operating at average temperatures of 1000 °C.

Nickel-based superalloys also have complex compositions, typically containing 10–20% chromium and with small additions of over 10 alloying elements that all contribute to the final microstructure. The primary matrix phase is known as the γ phase and is a continuous face centered cubic (FCC) austenitic phase. This matrix phase contains alloying elements including chromium, molybdenum, and cobalt that strengthen the alloy. The precipitate phase, γ' exists to significantly strengthen the alloy, aluminum and titanium additions cause γ' to coherently precipitate within the γ matrix phase (Stanners et al., 2020).

Interlayer bonding of nickel alloys is a relatively new process for researchers to look to optimize and improve. It has been referred to as a novel joining technique, and that is still an apt description, but many papers have been published on the successful joining of numerous nickel-based alloys; gaining constant improvements and a better understanding of the process over time. Diffusion bonding without an interlayer works well in pure materials with highly polished bonding surfaces, and even for certain dissimilar joints (Liu et al., 2013). However, even a good surface finish will have some surface asperities, which will lead to bond line porosity and sacrificed mechanical strength.

More traditional welding techniques such as gas-tungsten arc (GTA) have large heat-affected zones (HAZ) that generate differing microstructures to the base material, typically forming brittle intermetallics that reduced ductility and overall weaken mechanical performance (Hunziker et al., 1999). Even the currently most-optimized diffusion bonding processes also have HAZ, but they are much smaller, and the resulting microstructures can be better controlled than traditional methods, particularly by changing composition of the interlayer and bonding parameters (Torun and Celikyurek, 2008).

* Corresponding author.
E-mail addresses: 902545@swansea.ac.uk (W. Reeks), h.m.davies@swansea.ac.uk (H. Davies), Silvia.Marchisio2@Rolls-Royce.com, 902545@swansea.ac.uk (S. Marchisio).

https://doi.org/10.1016/j.jajp.2020.100030
Received 23 June 2020; Received in revised form 18 August 2020; Accepted 18 August 2020

Joining of dissimilar alloys to nickel-based alloys is just now beginning to gain interest, as the methods to do so have only recently been attempted (Aluru et al., 2008; Khakian et al., 2015). The literature focuses on interlayer bonding of various nickel-based superalloys, including single crystal variants, but will also include other nickel-based alloys, as research from those studies is undoubtedly useful and relatable.

Diffusion bonding/brazing process

Diffusion bonding involves the permanent joining of two faying surfaces via exposure to an elevated temperature over an extended period of time. The high temperatures allow for solid-state diffusion of atoms from each material into the other, physically bonding them together to form one component. Solid-state diffusion bonding is different to a similar process called diffusion brazing, which utilizes an interlayer that may become liquid state upon heating. No interlayers are used in standard diffusion bonding. Diffusion brazing is also known as transient-liquid-phase (TLP) bonding.

Solid-state bonding is strongly affected by the bonding time, bonding temperature, contact pressure, surface roughness and composition of interlayer if used (Stanners et al., 2020). Most bonds performed on nickel alloys utilize a high polish surface finish (Tarai et al., 2018). Typically, as surface roughness increases, bond integrity decreases, as the number of micro voids and pores formed in the bond increase. For nickel alloys, bonding temperatures of over 1000 °C are typically used. Higher pressures may be utilized to achieve the best contact between the faying surfaces.

In TLP bonding, the process is no longer entirely solid-state. Liquid forms at the bonding interface and wets the surfaces, spreading by capillary action. Temperature and bonding time are still as important, but now interlayer composition must be carefully considered as it has a large impact on the quality of the weld. Pressures used in TLP bonding are typically lower than those used in solid-state. The temperature of bonding is decided by the interlayer used, as this will determine when liquid will form at the interface.

There are now many proprietary nickel-based interlayers, such as: MBF30, Amdry- DF3, Niflex-110, which are specifically designed to join nickel alloys (Aluru et al., 2008; Wikstrom et al., 2006; Pouranvari et al., 2008). Some interlayers are designed to interdiffuse with the mating materials, forming a eutectic composition which melts at the bonding temperature, whereas others may already be in the eutectic/ peritectic phase which would melt also (Aluru et al., 2008; Khakian et al., 2015). Some interlayers are chosen as it is known that they will from certain compounds such as intermetallics upon heating, which may be essential to the strength of the joint.

Diffusivity between mating materials can be improved drastically by using certain interlayers, for example, nickel and copper are used frequently due to their ability to improve diffusivity between the faying metals, whilst remaining compatible to the joint. Copper has a thermal diffusivity approximately 10x that of steel at 25 °C (Akca and Gursel, 2015). It is vital that the interlayer is carefully chosen, as a poorly suited interlayer will detriment the joints significantly. The parameters that need to be considered can be found in the equation below describing the temperature dependence of diffusivity:

$$D = D_o e^{-Q/kT}$$

where

D = *diffusivity,* the coefficient of diffusion at the temperature T.
D_o = constant of proportionality.
e = Euler's number.
Q = activation energy required for diffusion.
T = activation temperature.
k = Boltzmann's constant.

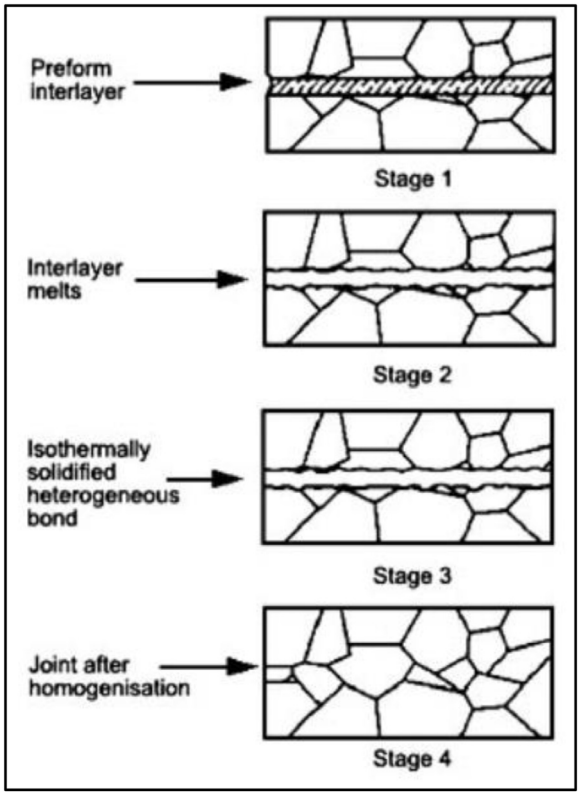

Fig. 1. Schematic for microstructural evolution in TLP bonding (Dunkerton, 2001).

The parameters Q, and T are very important as this will govern how easily the diffusion process will begin and thus how easily the metals will begin to join.

There are typically four major stages in TLP bonding: dissolution of the interlayer, liquid phase homogenization at the interface, isothermal solidification, and homogenization of the bond region. The diffusion coefficient is the driving force for the TLP process, and this changes from diffusion in the liquid phase, to solid-state diffusion in the latter part of the bonding process (Tuah-Poku et al., 1988). Fig. 1 shows a schematic of interlayer bonding.

Early studies by Tuppen et al. looked at the structural integrity of diffusion bonds on Ti-6Al-4V processed by a low-cost route. Resistance butt welds of the alloy were performed using a Gleeble thermomechanical simulator (Tuppen et al., 2006). Poor quality bonds were formed in air or partial vacuum owing to oxide formation, this was circumvented by incorporating a high vacuum into the bonding process. The microporosity within resistance bonds could be eliminated under sufficient bonding pressure and extended cycles. Time dependent creep will also encourage macroscopic plastic upset. Once optimized, the bonds had comparable tensile strength and ductility to conventional cross-rolled Ti-6Al-4V plate materials.

Before interlayer bonding was applied to nickel-based superalloys, the process was researched primarily on metals with lower melting points, such as titanium alloys (Chandrappa et al., 2018). The process developed at Swansea university, using powder-based interlayers to join Ti-6Al-4V, is outlined below.

The two parts to be bonded are held in the opposing sites of a servo-hydraulic rig via collets, with an interlayer attached to one of the titanium parts. The parts are brought into contact, so that the faying surfaces sandwich the interlayer. To avoid oxidation, the entire bonding procedure is performed in an argon chamber, which is contained in a quartz glass tube that surrounds the parts to be bonded, Fig. 2. The initial heating is provided by a water-cooled induction coil, where 900 °C is

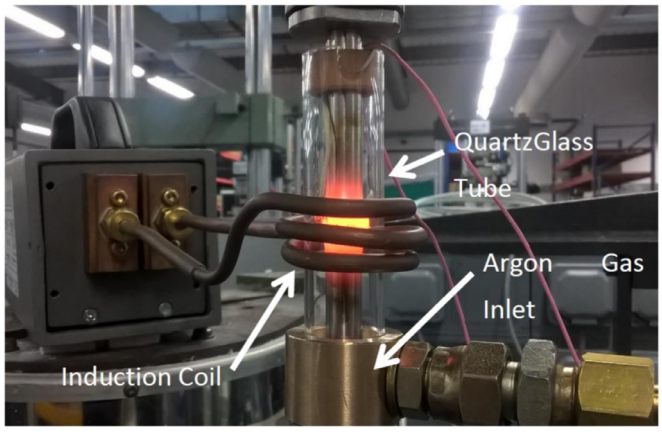

Fig. 2. Powder Interlayer Bonding setup for nickel-based superalloys at Swansea University (Stanners et al., 2020).

reached at a heating rate of approximately 6 °C/s. However, it is important to not exceed the bonding temperature, so a secondary heating rate of only 0.5 °C/s is employed to achieve the final temperatures. Bonding temperatures were held for 1 h. The bonded specimens were then allowed to air cool down to room temperature.

Type N thermocouples were welded to both faying parts, either side of the bond region (within 1 mm); and connected to a calibrated Fluke 54 II thermometer to accurately measure the temperature during the process. The maximum initial stress was 50 Mpa across the bond line for 60 min.

The interlayer utilized for the bonding of Ti-6Al-4V was made up of gas-atomized Ti-6Al-4V powder mixed with cellulose powder, glycerol and deionized water to create a paste which could be applied to one of the faying surfaces using a specially designed rig to ensure a consistent interlayer thickness of 100 μm (Davies et al., 2019).

Literature of diffusion bonding/brazing of nickel-based alloys

There are multiple types of interlayers that are utilised for improved joining of metals, the most common is a foil interlayer, where the components are condensed into a thin transportable layer that can be easily applied between the two faying surfaces. Typically, foils are made between 25 and 75 μm in thickness, though foil interlayers as thin as 2 μm have been utilised (Xiong et al., 2019). Proprietary interlayers are almost always foils, as these are the most stable and easiest to produce in larger quantities. Foil interlayers still allow for modification of the chemical composition to suit the particular alloys being bonded (Aluru et al., 2008).

Electroplating is also used to create interlayers and is ideal when a very thin interlayer is required. A disadvantage to electroplating is the restriction to only plating a single metal onto the surface of one of the bonding metals (Torun and Celikyurek, 2008; Yang et al., 2019). Typical thicknesses of an electroplated interlayer sit at 2–10 μm.

Powder-based interlayers are still relatively new. An advantage of these interlayers is that they can be made on-site with just the powder base and a few ingredients, however, they currently need to be made one at a time, directly onto one of the faying surfaces immediately prior to bonding. The powder interlayers are too fragile to be made in bulk and kept in storage for multiple subsequent bonds (Davies et al., 2019; Stanners et al., 2020). Another advantage is the customization capacity of the interlayer, where the composition of the interlayer can be easily modified to better suit the joining process. Flexible cloth interlayers have been athermally rolled from powder bases (Li et al., 2003).

For ease of access, Table 1 shows a summary of the materials, interlayers, bonding parameters, mechanical properties, and remarks taken from the applicable studies featured in this review.

Foil/composite interlayers

Foil interlayer, GH4099: A study by Xiong et al. (2019) investigated the diffusion bonding of GH4099 nickel superalloy with pure nickel foil interlayers of different thicknesses. It was found that decreasing the interlayer thickness resulted in more homogenous element distribution and hardness across the joint interface. The ideal bonding conditions for recrystallization with minimal grain coarsening were found using a 2 μm thick pure nickel interlayer at 1120 °C for 90 min.

The 38 mm diameter cylindrical specimens were diffusion bonded under 4 MPa at 1120–1160°C for 60–120 min and allowed to cool to room temperature in a vacuum furnace (5×10^{-3} Pa). The solution treatment temperature of GH4099 is 1100–1160 °C, and this decided the bonding temperature as to allow for sufficient atomic diffusion, whilst avoiding rapid grain coarsening.

The microstructure of the as received material contained some large blocky carbides of MC and many small carbide particles of $M_{23}C_6$ distributed at grain boundaries or in grains. Annealing twins were also present. The mean diameter of the γ grains was about 36 μm. The microstructure of the joint directly diffusion bonded without the presence of an interlayer had a very apparent bond line, which consisted of the $M_{23}C_6$ precipitates and microvoids produced by the initial surface roughness of the faying surfaces. The integrity of the joint was severely impaired and fractured along the joining interface when the specimens were being machined post-bonding.

The microstructure of the interlayer bonded specimens varied with bonding time and temperature, with the largest grains forming with the higher time and temperature bonds. A carbide depleted zone formed around the interlayer, due to the increased solubility of C in Ni at the bonding temperature. The initial carbides present in the base material diffused into the pure nickel interlayer after decomposing during the bonding process, the diffusion into Ni is driven by chemical potential gradient. Microvoids were present in the interlayer bonded specimens, and their significance increased with interlayer thickness. The 2 μm interlayer joint had the least number of microvoids, the largest γ' and the most uniform element distribution and was therefore selected to optimize the bonding parameters.

Plasticity, elongation and fracture toughness of the bonded joint were improved by use of a pure Ni interlayer, with the best result having an elongation of 32% (107% of base metal) and an absorbed energy of 47 J (89% of base metal).

Perhaps the best testament to the strength of the interlayer bonds formed was that the joint fractured at the base metal when using ideal bonding parameters and a pure Ni interlayers, unlike the joints without an interlayer which fractured at the joint interface during machining (Xiong et al., 2019).

Amdry DF-3 Foil interlayer, IN738LC: Transient liquid phase bonding of IN 738LC superalloy with an Amdry DF-3 interlayer was investigated by Wikstrom et al. (2006). The effect of bonding temperature and time on the microstructure was observed. The interlayer gap width was 75 μm, and bonding was carried out between 1120 and 1225 °C for various time. TLP bonding was performed under vacuum (10^{-4} Torr to 10^{-5} Torr) in a LABVAC II brazing furnace.

It was found that increasing the time spent at brazing temperature increased the extent of isothermal solidification of the liquidated filler metal. Complete isothermal solidification occurred within a 12 h holding time at 1175 °C, and this precluded formation of centreline eutectic. Increasing the brazing temperature to 1190–1225 °C led to an increased amount of liquid and subsequent eutectic at the joint than that present after an equivalent holding time at lower temperatures (1120–1175 °C); this was a deviation from predictions by TLP diffusion models. Precipitation of chromium rich particles was observed in the base metal regions adjacent to the joint interface. Increasing the diffusion brazing temperature resulted in a considerable decrease in the extent of interface precipitation, which would increase strength and ductility of the bonded

Table 1
A summary of components taken from the studies featured in this review.

No.	Ideal Bond Parameters	Parent Materials	Interlayer Materials	Strength (MPa)/ Mechanical Properties Noted	Interface Hardness (HV)	Summary + Remarks	Ref.
1	1120 °C for 90 min under 4 MPa	GH4099	Pure Ni, Foil, 2 μm	89% of base metal energy absorption, 107% elongation	n/a	Bonds fractured at the base metal when using ideal bonding conditions and a pure Ni interlayer. Microvoids became more significant with increased interlayer thickness.	(Xiong et al., 2019)
2	1120–1225 °C for various times (no ideal found)	IN738LC	Amdry DF-3 foil, 75 μm	n/a	475	The DF-3 filler alloy can obtain a balance between the formation of interface chromium rich particles and a re-occurrence of the centreline eutectic. Increasing the brazing temperature decreased the extent of interface precipitation	(Wikstrom et al., 2006)
3	1200 °C for 8 h under 0.3 MPa	DD6 Single Crystal	Composition range of 1 ≤ Cr ≤ 2, 2.5 ≤ *W* ≤ 4, 3 ≤ Co ≤ 4.5, 1.5 ≤ Al ≤ 3, 0.5 ≤ Mo ≤ 1, 3 ≤ *B* ≤ 3.6. 40 - 60μm	n/a	n/a	This investigation was primarily a study of creating the ideal interlayer material for bonding DD6. Bonding at 1200 °C instead of 1070 °C reduced the number of brittle borides in the diffusion zone.	(Zhai et al., 2014)
4	1100 °C for 75 min, followed by 1150 °C for 240 min homogenization	GTD-111	MBF30 (Ni-Si-B amorphous interlayer) foil	n/a	n/a	Crack-free joint regions were obtained via complete isothermal solidification and lower bonding temperatures. It was concluded that further study is needed to achieve a joint with similar microstructure to the base metal	(Pouranvari et al., 2008)
5	1160 °C for40 min	Hastelloy X	Ni-Cr-B-Si-Fe AMS 4777 foil, 35 μm	65 MPa, 69 J energy absorption	350	All bonds were deemed acceptable, with joint efficiencies all being > 82%. The fracture origin for all samples was around the DAZ, to improve mechanical properties further, reducing the amount of precipitates in the DAZ would be necessary	(Malekan et al., 2019)
6	1240 °C for 12 h followed by PBHT 1305 °C for 4 h	Rene' N5 Single Crystal	Ni-Cr-Co-Mo-W-Ta-Re-B amorphous foil	81.5% Shear strength of the base metal	No obvious hardness variation	No pores or cracks observed at the interface pf the TLP joint with or without a PWHT. White precipitates, found to be nickel-rich borides, these were eliminated by the PWHT.	(Guo et al., 2017)
7	1100 °C for 30 and 60 min, followed for homogenization at 1206 °C for 1 and 2 h	Rene 80	Ni-Cr-Si-B-Fe-C alloy, 50 μm foil	810 vs 840 of base alloy	480 at 1 h, 610 at 2 h of homogenization	Voids were formed when bonding under argon conditions, due to the presence of argon impurities, vacuum bonding removed impurity problem.	(Ekrami et al., 2007)
8	1270 °C for 48 h	Mar-M247 Single Crystal	Ni-Cr-Co-W-Ta-B, 50 μm foil	n/a	n/a	Mechanical analysis of the bonded specimens is needed to test for suitability of the process. Bonds free of brittle phases in the single crystal alloy were obtained, and based on the microstructure one would expect good mechanical strength	(Zheng et al., 1993)
9	1150 °C for 240 min	Mar-M247 Polycrystal	Ni-Cr-Co-W-Ta-B, 50 μm foil	450	290	Bonds performed for 1 and 60 min were significantly harder and more brittle than the 240 min bond. PBHT were recommended for further improvement to mechanical properties.	(Liu et al., 2017)
10	1000 °C for 4 h	Nickel Aluminide	Pure Ni electroplate, 10 μm	97% of base alloy	290 vs 350 of base metal	Hardness in the bond region actually got softer, attributed to the lack of aluminum atoms available at the bond center. More microstructural analysis via EDS or EBSD would be useful for compositional analysis	(Torun and Celikyurek, 2008)
11	1050 °C for 60 min under 20 MPa	Ni3Al-based alloy	Pure Ni electroplate, 3 μm	617	n/a	Although raw diffusion bonding could achieve a sound bond, the use of a pure nickel electroplated interlayer managed basically the same shear strength at a lower bonding temperature.	(Yang et al., 2019)

(*continued on next page*)

Table 1 (*continued*)

No.	Ideal Bond Parameters	Parent Materials	Interlayer Materials	Strength (MPa)/ Mechanical Properties Noted	Interface Hardness (HV)	Summary + Remarks	Ref.
12	1100 °C for 5–10 min under 5–10kN	RR10XX	RR10XX, 100 µm powder-based	n/a	480 - 560	Grains were refined beyond that of the base material, which increased hardness in the bond region. Mechanical testing is recommended for further study	(Stanners et al., 2020)
13	1050 °C for 60 min	IN718	Ni-Cr-Fe-Si-B powder-based, 50 µm	n/a	n/a	Boron diffusion resulted in the formation of brittle borides at the diffusion-affected zone. This would need to be alleviated to achieve sound mechanical performance. An investigation into the effect of PBHT is recommended	(Tarai et al., 2018)
14	1250 °C under 5.58 × 10–3 MPa, plus 35 h PBHT	Ni-based single crystal superalloy	Ni–Cr–Co–W–Mo–B alloy cloth	n/a	n/a	The study focused primarily on developing a flexible, easy to use interlayer cloth. After isothermal solidification, a fully homogenized bond was achieved. Crystallographic orientation must be maintained in both mating halves to preserve single crystal growth	(Li et al., 2003)
15	1180 °C for 64 min	IN738LC to Nimonic 75	MBF-80 foil, 75 µm	n/a	n/a	The study used modeling to predict the final microstructure and time to complete isothermal solidification. The microstructures of the isothermally solidified bonds looked sound, but mechanical testing is still required.	(Khakian et al., 2015)
16	1130 °C for 100 min plus homogenization HT	FSX-414 (cobalt based) to GTD-111	MBF-30 foil, 50 µm	527.9	695	Homogenization treatment was complete at 1150 °C for 4 h. This allowed the specimens to achieve complete isothermal solidification. There are still considerable shear strength gains to be made with the bonded specimens.	(Hadibeyk et al., 2018)
17	1050 °C for 45 min plus homogenization HT at 1180 °C for 180 min	IN718 to IN600	MBF-20 foil, 50 µm	568	210	PBHT completely removed the intermetallic compounds formed during bonding. Bonds performed over 45 min had reduced hardness but large variation across the joint.	(Jamaloei et al., 2017)
18	1190 °C for 120 min	DD98 single crystal to K465	Ni-12Cr-3B foil, 40–60 µm	n/a	n/a	Isothermal solidification did not complete, leaving multiple phases from the residual liquid interlayer.	(Liu et al., 2011)
19	1190 °C for 240 min under 2.7 MPa	DD98 single crystal to M963	Ni-15Cr-3B amorphous alloy foil, 40–60 µm	Creep rupture performance comparable to M963 base material, at 800 °C/350 MPa	n/a	Due to the difference in the diffusion coefficient of melting point depressants, there is a dissymmetry of bonding line when joining the two alloys. Hardness data would show key variances across the joint	(Liu et al., 2010)
20	Laser welding, 90 A, 10 ms, 6 Hz	Ti3Al to Ni-based superalloy	Pure titanium foil, 0.4 mm	177 MPa, 0.4% elongation	650–850	Even after post-weld heat treatment, joints fractured at the weld interface due to the presence of intermetallics, specifically Ti2Ni. Joints were significantly improved over raw diffusion bonds.	(Cai et al., 2018)
21	800 °C for 60 min under 50 MPa	IN718 to gamma TiAl	Nano-sputtered, Ni/Al, 5 and 14 nm	n/a	n/a	The study shows that nano-sputtering an interlayer can be used to drastically improve the joint quality along the central region of the bond. No mechanical testing was performed.	(Ramos et al., 2008)
22	1200 °C for 120 min	IC10 single crystal to GH3039	BiNi2 foil, 50 µm	750 at room temperature, 220 at 900 °C	375	Due to the difference between the microstructure of the base metals, the TLP bonding joint exhibits bonding asymmetry	(Zhang et al., 2016)
23	1150 °C for 10 min, plus 1000 °C for 100 h PBHT	MM247 Ni3Al to NiAl-Hf single crystal	Ni3Al-Cu powder mesh, approx. 200 µm	Bonds exhibited parent material shear strength	250 - 350	Failure occurred in the bulk substrate rather than at the interface. A PBHT was necessary to achieve the impressive bond strengths.	(Gale and Wen, 2001)

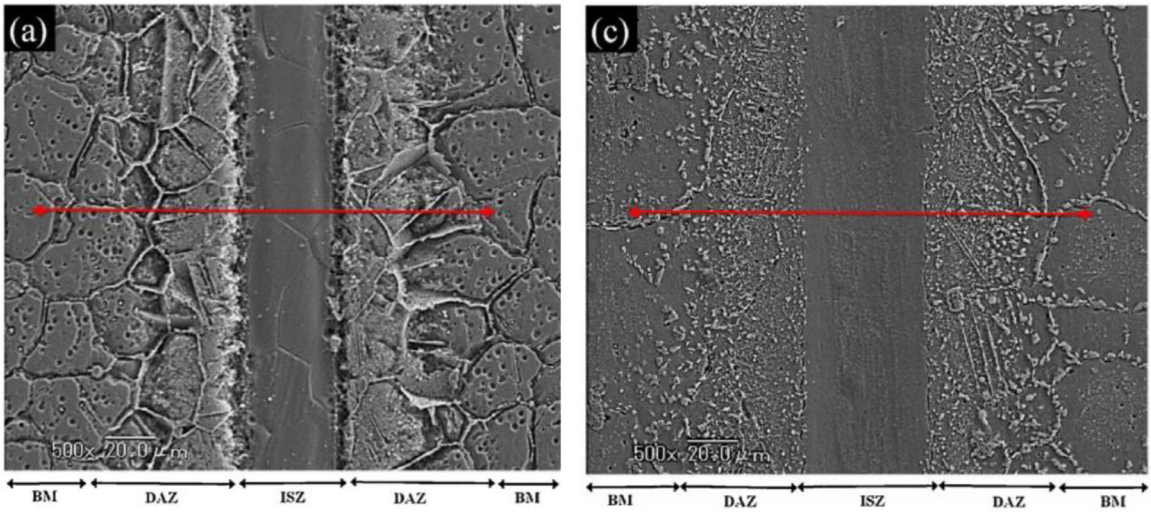

Fig. 3. SEM microstructures of joints bonded at (a) 1070 ˚C and (c) 1160 ˚C (Malekan et al., 2019).

alloys, though no mechanical testing was complete on the bonded alloy (Wikstrom et al., 2006).

Foil interlayer, DD6 SX superalloy: Zhai et al. (2014) conducted research on interlayer alloys for TLP bonding of single crystal nickel-based superalloy DD6. Interlayer foils were developed, with thickness 40–60 μm, they were prepared using a single roller rapid solidification apparatus. The microstructures of the prepared interlayers were fine and homogeneous. The TLP welding process was completed at 1200 ˚C, for 8 h, with a welding pressure of 0.3 MPa, under a vacuum at 5×10^{-2} Pa. Specimens were cooled to room temperature within the furnace.

The investigation focused on whether or not the developed interlayer would be sufficient for the bonding process, the microstructure and wettability on the substrate of the interlayer alloy were investigated. Maintaining the single crystal structure of the alloy was a key issue that needed to be addressed. The primary challenge of the investigation was achieving complete isothermal solidification in the bond line as to remove the brittle precipitates that form with insufficient bonding time.

The microstructure of the bonded joint was found to be consistent with the base metal, and the joint was composed of three distinct zones: weld center zone, isothermal solidification zone, and the diffusion affected zone. Within the joint, elemental diffusion was sufficient and boride formation was minimised in the diffusion zone. To achieve single crystal growth, the crystallographic orientation had to be maintained in both mating halves (Zhai et al., 2014).

Foil interlayer MBF30, GTD-111: TLP bonding of GTD-111 nickel-based superalloy using Ni-Si-B amorphous interlayer, MBF30 was investigated by Puranvari et al. (2008). Bonding was performed at 1100 ˚C with different holding times under vacuum. Microstructural studies showed that before completion of isothermal solidification, the bond region consists of four distinct zones: centreline eutectic structure due to athermal solidification, solid solution phase due to isothermal solidification, diffusion-induced boride precipitates and base metal.

The remained liquid phase after an incomplete isothermal solidification at the bonding temperature transformed on cooling to non-equilibrium eutectic structure consisting of γ-solid solution phase and nickel-rich borides. Increasing the bonding time led to a decrease in the amount of eutectic structure, and complete isothermal solidification occurred at a bonding time of 75 min. Homogenization of isothermally solidified bond at 1150 ˚C for 240 min resulted in reducing of secondary precipitates within the DAZ and formation of significant γ' precipitates in the bond region.

It was concluded that further study is needed to achieve a joint with similar microstructure to that of the base metal (Pouranvari et al., 2008).

Foil interlayer, Hastelloy X: Malekan et al. (2019) studied the effect of bonding temperature on the microstructure and mechanical properties of Hastelloy X superalloy joints bonded with a Ni-Cr-B-Si-Fe foil interlayer. Bonding was achieved at 1070–1160 ˚C in a vacuum furnace.

Isothermal solidification was completed for all samples after 40 min of transient liquid phase bonding. The isothermally solidified zone was composed of Ni-rich solid solution γ phase. The Ni-rich boride and binary Ni-Si eutectic were observed in the centreline of the sample bonded at 1070 ˚C for 5 min. Precipitate density at the DAZ increased with increasing temperature. Fig. 3 shows the difference in microstructure based on bonding temperature. High microhardness values observed in the DAZ were attributed to the presence of borides. A decrease in the volume fraction of borides and the development of rounder morphologies with increasing T_b up to 1160 ˚C resulted in increasingly uniform microhardness distributions across the joints. 1160 ˚C bonds showed the highest shear strength, failure energy, and maximum strain, while the lowest values observed for the samples prepared at 1110 ˚C were attributed to its high density of DAZ borides and low degree of solid solution strengthening. However, the shear test strengths for all samples were considered acceptable, with joint efficiencies of > 82%.

It was proposed that the mechanical properties of the bonded alloy could be improved by reducing the fraction of the precipitates that form in the DAZ (Malekan et al., 2019).

Foil Interlayer, Rene' N5 SX: TLP bonding of nickel-base single crystal alloy Rene' N5 using a novel Ni-Cr-Co-Mo-W-Ta-Re-B amorphous interlayer was investigated by Guo et al. (2017). Bonding was performed in a vacuum furnace at 1240 ˚C for 12 h, and was followed by a post-weld heat treatment at 1305 ˚C for 4 h. The shear strength and microstructure of the joined alloy with a PWHT was compared to the base metal and to bonded specimens without a PWHT. The wetting of the interlayer was also studied in depth.

No pores and cracks were observed at the interface of the TLP joint with or without a PWHT. Few white precipitates were found at the centreline of the joint of the no PWHT sample, EDS analysis showed these to be nickel-rich boride phases due to the low solubility of boron in the nickel-base superalloy. These borides are brittle and detrimental to the mechanical properties, which was seen in the shear strength and hardness data, where the hardness was 50 Hv higher than the base metal, but shear strength was at 66.8% of the base metal. After the PWHT, relatively uniform chemical element distribution was attained, and no obvious hardness variation was observed across the joint. The shear strength of the PWHT bond was 81.5% of the base metal, which can be attributed to the increase of volume fraction of γ' phase in the bonding region.

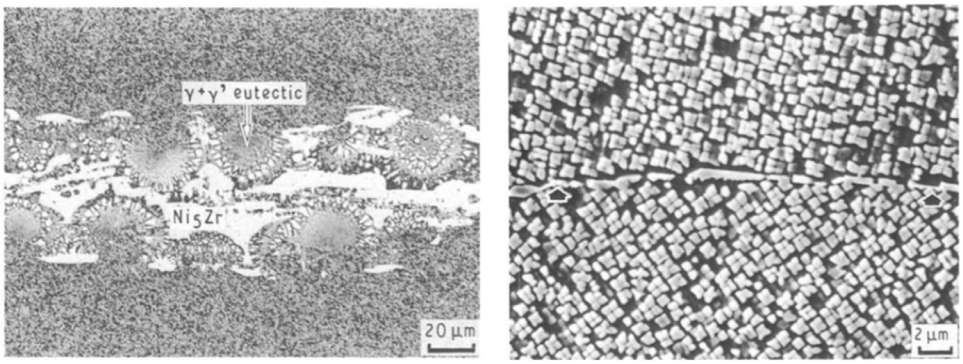

Fig. 4. (left) Microstructure of the bond after 1270 °C for 8 h, (right) microstructure after 1270 °C for 48 h (Zheng et al., 1993).

The amorphous interlayer exhibited excellent wettability on the single crystal nickel superalloy (Guo et al., 2017).

Foil interlayer, Rene 80: The effect of transient liquid phase diffusion bonding on the microstructure and properties of nickel base superalloy Rene 80 using a Ni-base interlayer has been investigated by Ekrami et al. (2007). The interlayer used was a Ni-Cr-Si-B-Fe-C alloy, set to a thickness of 50 μm. Bonding was achieved at 1100 °C for 30 and 60 min in an argon gas atmosphere and under vacuum, specimens were cooled to room temperature before homogenization at 1206 °C for 1 and 2 h.

Voids and porosity were observed in the bond region of the bonds made in the argon atmosphere. Formation of these voids were related to the presence of argon impurities. Intermetallic compounds were seen at the joint region, these phases were removed via the homogenization heat treatment. Hardness of the bond region was greater than the hardness of the parent alloy due to the higher content of depressant elements at the bond region. Increasing the bonding time decreased the hardness of the bond region to the parent alloy hardness level. Shear strength of the bonds made under vacuum was greater than the argon atmosphere bonds, due to the formation of voids in the argon atmosphere bonds. The shear strength of bonds made in vacuum and then homogenized at 1206 °C for 2 h was much closer to the shear strength of the parent alloy (Ekrami et al., 2007).

Foil interlayer, SX superalloy: An investigation into the TLP bonding of a single-crystal nickel superalloy using a custom interlayer was completed by Zheng et al. (1993). It is notoriously difficult to weld single crystals whilst retaining the majority of the material strength, so an effort was made to find an interlayer material which could allow successful high integrity joining. After much analysis and experimentation, the composition for the interlayer was chosen as: Ni-10Co-8Cr-4W-13Zr.

Using zirconium in the interlayer was of large focus as it was an unknown in the bonding of single crystal nickel alloys, but its very positive effects on the strength, ductility, and low cycle fatigue of directionally solidified superalloys were understood. Using this alloy as a 50 μm thick interlayer, bonds free of brittle phases in the single crystal superalloy were obtained by isothermal solidification at 1270 °C for 48 h, Fig. 4. Bonds performed for 8 h had drastically different microstructures, containing eutectic and a distinct lack of γ'. There was still a noticeable bond line, due to a grain boundary formation by the two pieces of single crystal with different orientation, but the remaining microstructure had identical morphology to that of the base metal (Zheng et al., 1993).

Foil interlayer, Mar-M247: Liu et al. (2017) investigated the microstructural evolution and mechanical properties of TLP bonded joints of Mar-M247 superalloys using a Ni-Cr-Co-W-Ta-B interlayer. Bonding was performed in a vacuum furnace at 1150 °C for 1, 60, 120, and 240 min. Specimens were cooled in air to room temperature. With increasing bonding time, alloying elements diffused across the joint zone and formed a solid solution and intermetallic compounds. Dendritic formation and solute partitioning governed the microstructure development. The bond performed at 1150 °C for 240 min had the greatest tensile strength and reached complete isothermal solidification. After complete isothermal solidification, microhardness of the joints was more homogeneous. The refractory elements present in the Ni-Cr-Co-W-Ta-B interlayer made complete isothermal solidification more difficult. Post-bond heat treatments were recommended to further improve the final bond properties. (Liu et al., 2017)

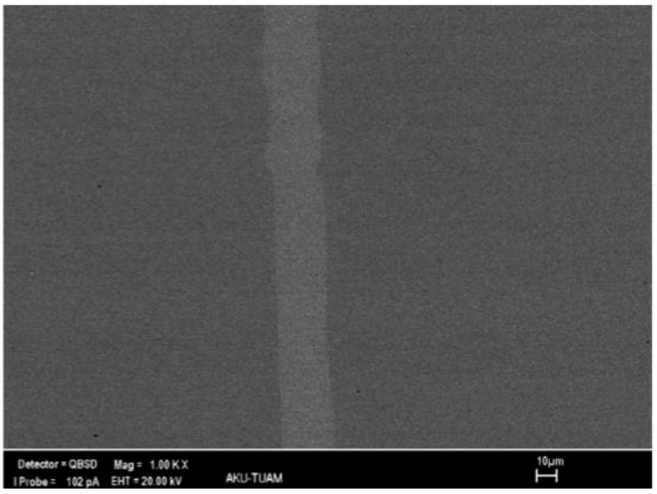

Fig. 5. SEM back-scattered electron micrograph showing sound, void-less bonding after 4 h (Torun and Celikyurek, 2008).

Electroplated interlayers

Electroplated, Ni3Al: Nickel aluminides are of particular interest for high temperature applications due to their oxidation resistance and excellent mechanical properties. Torun and Celikyurek (2008) investigated interlayer bonding of the alloy. Weldability is an issue, as earlier studies that focused on gas-tungsten arc (GTA) and electron beam welding (EB) confirmed the susceptibility to HAZ cracking and solidification cracking. So, an investigation into the effect of interlayers on the diffusion bonding was launched. Using a pure nickel interlayer, all bonded samples exhibited sound bonding without any micropore and microcracks along the interface, Fig. 5. EDS analysis showed that aluminum atoms in from the matrix migrated into the nickel interlayer, with the percentage of Al in the interlayer increasing with increasing process time.

In order for the shear strength of the bonded samples to be compared to the base material, the specimens were annealed at 1000 °C for 4 h. The interlayer bond region was softer than that of the base aluminide due to the reduced aluminum content, but shear strength of the 4-h interlayer bond was 97% of the base alloy shear strength (Torun and Celikyurek, 2008).

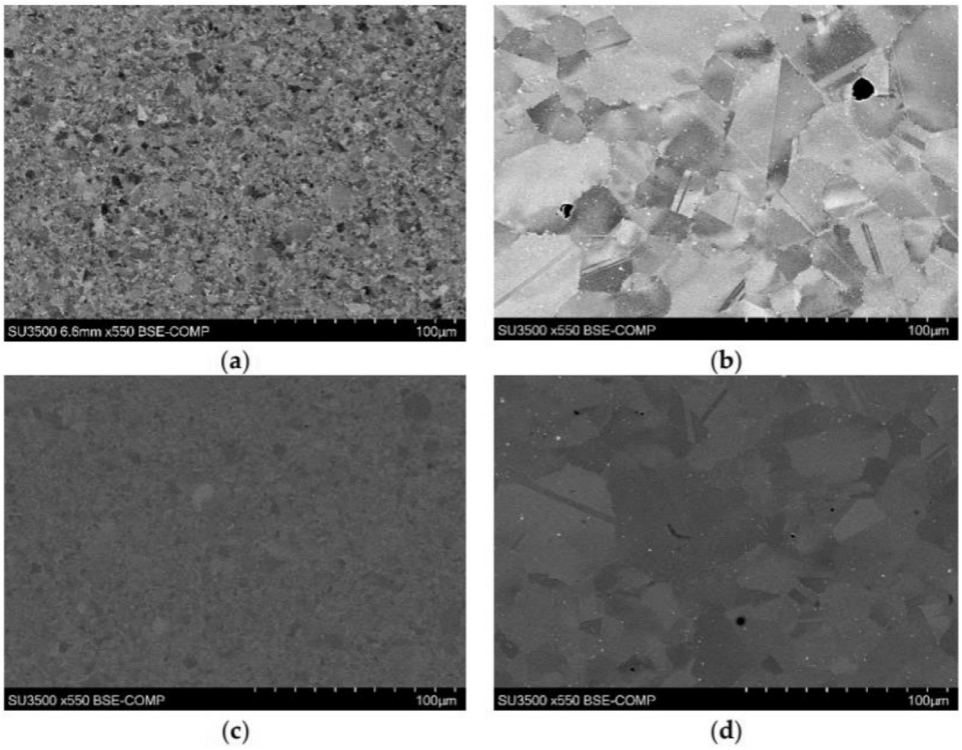

Fig. 6. SEM images of (a) bondline of (b) base material. (c) is the bondline of (d) base material. A much finer grain size is seen in the bonded material. (Stanners et al., 2020).

Foil and Electroplating, Ni_3Al-based alloy: Diffusion bonding of Ni_3Al-based alloy using a pure Ni foil interlayer was investigated by Yang et al. (2019). Bonds were performed at 950–1100 °C for 10–60 min under a pressure of 20 MPa, and the shear strengths of the various joints were compared. The maximum joint strength achieved for the diffusion bond without an interlayer was 689 MPa, with the parameters of bonding being 1100 °C for 600 min at 20 MPa; this corresponded to an interface bonding ratio of 95%. However, the fracture surface of the bonded joint was characterized primarily by cleavage fracture, indicating that the specimen failed via brittle rupture. This was caused by the coarsening phenomenon of γ' precipitates. To inhibit this, pure Ni interlayers were used, a 30 μm foil, and a 3 μm thick electroplated Ni coating. Bonding was achieved at 1050 °C, and it was found that the 30 μm thick foil interlayer completely disappeared due to interdiffusion with the Ni_3Al base alloy; the performance of the joint was inferior to that of the base metal due to the heterogeneity in the diffusion zone. When bonded with the 3 μm thick electroplated coating, the microstructure of the diffusion zone was consistent with that of the base metal, and shear strength equalled that of the direct diffusion bonded joint at 1100 °C. Fracture morphology changed from cleavage fracture to alternating dimples and facets (Yang et al., 2019).

Powder interlayer bonding

Powder interlayer, RR10XX: Stanners et al. (2020) looked at the effects of changing temperature, force, and time of the bonding process on the microstructure, porosity, and hardness of the joined alloy. The study was on the latest generation nickel-based superalloy from Rolls-Royce, using a 100 μm thick interlayer of the same composition. It was found that at higher temperatures of bonding (1100 °C), more recrystallization occurred, resulting in a change in the microstructure from the starting base material. Recrystallization in the bond region lead to a more refined grain size than in the base material, which lead to an increased hardness value, as supported by the Hall-Petch relationship (Stanners et al., 2020).

Bonding was performed in using an induction coil to provide the heating, and a quartz glass tube to facilitate an argon gas shield to prevent oxidation, Fig. 1. Temperatures of bonding varied between 1000 and 1100 °C, and contact forces of 5–10 kN were applied. Most bonds were performed over a 5–10 min period, but some were kept at an elevated temperature for an additional 30 min, with a reduced force of 0.5 kN. Fig. 6 shows the finished microstructures of the various bonds performed.

Powder interlayer, IN718: Tarai et al. (2018) successfully bonded nickel-based superalloy IN718 via TLP bonding using a Ni-Cr-Fe-Si-B interlayer. The interlayer material was developed via the mechanical alloying (MA) process in a high-energy planetary ball mill. After 50 h of milling, the equiaxed alloy powders reached 12 μm in size. This experimental interlayer material had a melting temperature of 1025 °C, 25 °C lower than the commercially available interlayer material BNi-2.

The TLP bonding process was achieved at 1050 °C held for one hour, the bonded specimens were subsequently furnace cooled to room temperature. The bond region had three distinct zones: bonded zone, diffusion affected zone, and base metal zone. Diffusion of boron from the interlayer to the base material resulted in isothermal solidification during the TLP bonding, resulting in the formation of borides at the diffusion-affected zone (Tarai et al., 2018).

Cloth interlayer, single crystal Ni superalloy: Li et al. (2003) experimented with a nickel interlayer alloy for joining a nickel-based single crystal superalloy. The Ni-Cr-Co-W-Mo-B interlayer alloy was specifically designed for bonding single crystal nickel alloys. The < 45 μm powder was thermally rolled into a flexible insert alloy cloth by mixing with an organic compound, which disappears upon heating. This flexible interlayer cloth was inserted between the faying single crystal surfaces.

The bonding process utilized a bonding pressure of 5.58×10^{-3} MPa at a temperature of 1523 K. These parameters meant the process was transient liquid phase, meaning the cloth interlayer melted during the process. The bonding times were varied, and post-bond heat treatments were used. Fig. 7 shows the difference in microstructure caused by bonding time.

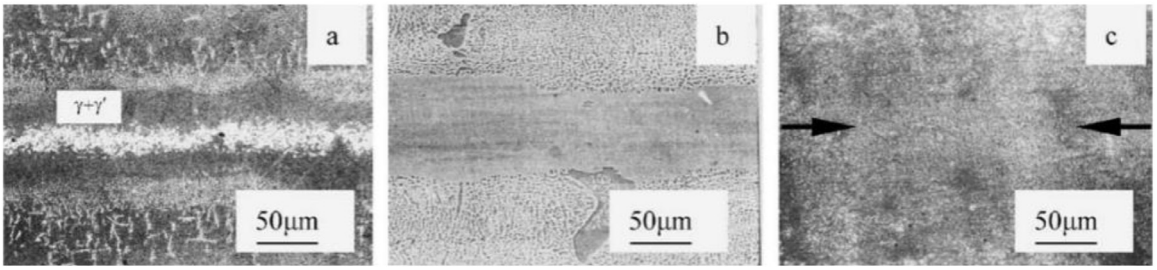

Fig. 7. SEM images of TLP bonds (a) bond made at 1220 °C for 1 h, (b) bond made at 1220 °C for 35 h, (c) fully homogenized bond at 1220 °C for 35 h followed by solution and aging treatments (Li et al., 2003).

The interlayer had similar composition to the base metal being joined, with a couple of important distinctions. Boron was added to the filler material to act as a melting point depressant, and the amount of boron is controlled to obtain the optimum balance between melting point and ease of subsequent homogenization. The single crystal superalloy was γ' strengthened, meaning it had titanium and aluminum in its composition. These elements are left out of the filler material and are allowed to diffuse into the joint region from the base material to form the stable, strengthening precipitates.

The crystallographic orientation of the single crystal was [001], and this orientation was always aligned perpendicularly to the joint interface.

The study found that an insufficient bonding time led to M_3B_2 precipitates forming both in the center of the joint and in the diffusion layers. TLP bonds free of these brittle phases were obtained by isothermal solidification at 1220 °C for 35 h. To achieve a fully homogenized bond in the superalloy, a post-bond heat treatment was required (Li et al., 2003).

Literature on interlayer bonding of dissimilar nickel alloys

There are numerous challenges associated with dissimilar bonding, perhaps the most complex to overcome is the formation of unwanted compounds at the bond region. Careful analysis of diffusivity and chemical reactivity of the elements involved is needed to find the most suitable interlayer for the dissimilar bond (Aluru et al., 2008). Bonding one nickel alloy to a different nickel alloy has become much easier in recent years, with commercially available interlayers designed for that exact purpose being an option. But bonding a nickel alloy to a completely different alloy, say titanium, often requires much more consideration when choosing the interlayer. The use of composite interlayers that have alternate elements on each side have been developed for certain dissimilar bonds (Cai et al., 2019).

*Foil Interlayer, CMSX-4 SX to IN739 and IN939:*Aluru et al. (2008) investigated the TLP bonding of dissimilar nickel-based superalloys, specifically focusing on the wettability of the various substrates. The alloys in question were the single crystal superalloy CMSX-4, and two polycrystalline superalloys, IN 739 and IN 939. The use of nickel composite interlayers Niflex-110 and Niflex-115 were compared with conventional BNi-3 brazing foils.

The TLP bonding process was performed in a tube furnace under a vacuum at 1160 °C. The interlayers used were 50 μm in thickness. Post-bond heat treatments (PBHT) were performed on the as bonded samples to allow more diffusion of aluminum from the substrates, allowing more γ' to form on the bond line. The level of formation of γ' was the dominant factor in the room temperature shear strength of the bonds. It was found that a greater amount of γ' formed in the bond region of the CMSX-4 – IN 939 joints when compared to that of CMSX-4 – IN 738; this was unexpected as IN 939 is lower in aluminum and higher in chromium than IN 738. It was assumed that the presence of other γ' formers and γ stabilizers influenced the overall behavior of the bonds.

The average peak shear stresses of the bonded alloys were compared. It was found that the CMSX-4 – IN 939 joints out-performed the CMSX-4 – IN 738 joints, especially without a post-bond heat treatment where the greater amount of γ' formed in the joint greatly improved strength. The peak shear stresses after a PBHT were near-identical to each other, but still lower than that of the as-received material. The formation of secondary phases in the diffusion zone of the polycrystalline substrate, led to the formation of brittle secondary cracks, reducing shear stress. The Niflex foils displayed porosity, but this had no apparent effect on the shear strength of the bonds. (Aluru et al., 2008)

*MBF-80 foil interlayer, IN738LC to Nimonic 75:*Khakian et al. (2015) completed a study on the effect of bonding time on the microstructure and isothermal completion during TLP bonding of dissimilar nickel-based superalloys IN738LC and Nimonic 75. MBF-80 interlayers were used, with the composition Ni-15Cr-3.5B and thickness of 75 μm. The TLP process was performed using an electrical furnace at temperatures between 1080 °C and 1180 °C, under a vacuum of 10^{-5} mbar. Bonding time varied from 5 to 180 min. Heating rate was set to 20 °C/min after 950 °C was reached. It was found that increasing the bonding time at a constant temperature, the eutectic structure formed in the centreline first loses its continuity and then is eliminated. If there was not enough time for isothermal solidification, the remaining liquid would transform to γ-eutectic, Cr-rich boride and Ni-rich boride through a binary and ternary eutectic transformation. It was found that there is a reverse relationship between the thickness of the athermally solidified zone and bond strength (Khakian et al., 2015).

MBF-30 Foil interlayer, FSX-414 (cobalt based) to GTD-111: Cobalt-based superalloys are used for the first stage nozzles in gas turbines, and like Ni-based superalloys, they are susceptible to microcracking during welding. The dissimilar TLP joining of Co-based superalloys FSX-414 to Ni-based superalloys GTD-111 was investigated by Hadibeyk et al. (2018).

The interlayer used was a 50 μm thick Ni-Si-B amorphous filler material, known as MBF30. The interlayer was in the form of a foil. No additional pressure was applied during the TLP bonding process, just the applied weight of the coupons and assembly fixture. The temperature of the vacuum furnace used for bonding was chosen as 1130 °C, and bonding times varied from 45 to 100 min, Fig. 8 shows the effect of bonding time on microstructure. Joined specimens were allowed to cool to ambient temperature in the furnace. Homogenization heat treatments were applied at 1150 °C for 4 h, to obtain a more uniform microstructure in the bond region.

It was found that increasing the bond time led to a slight increase in shear strength, reaching a peak of roughly half the shear strength of the base GTD-111 alloy at 100 min bonding time. Hardness across the joint was non-uniform without a PBHT, spiking in value at the athermally solidified zone, and also increasing in the diffusion affected zone. These zones acted as crack nucleation sites in the TLP bonds. It was found that increasing the bond time made the hardness across the joint more uniform, as it allowed for complete isothermal solidification. The increase in shear strength of the 100 min bonds was related to the solid solution strengthening and removal of eutectic phase at the bond line. The

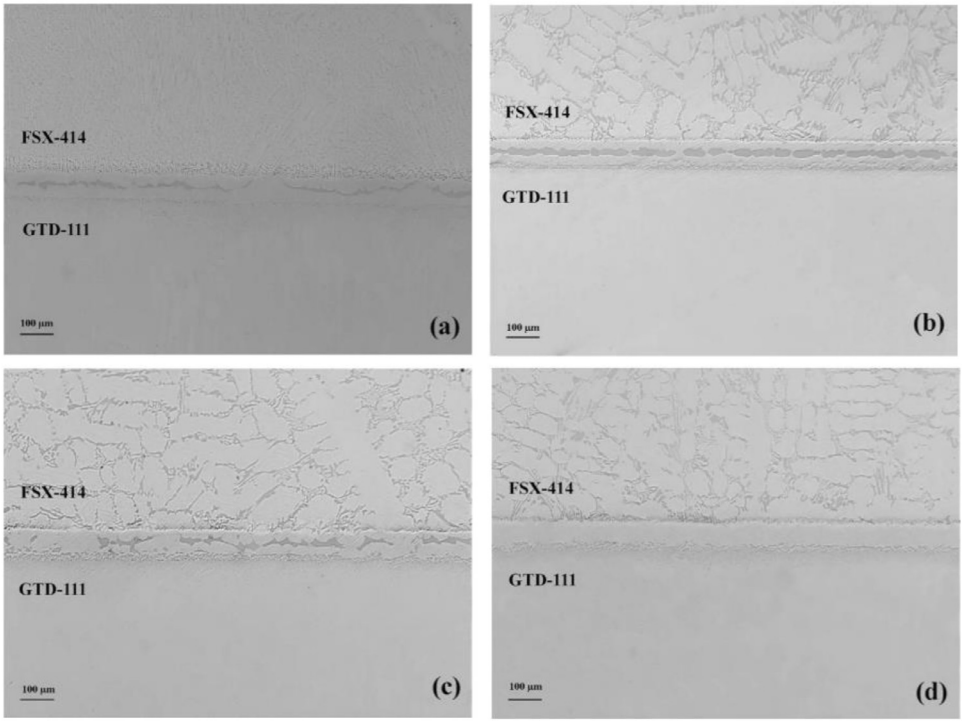

Fig. 8. SEM images of the bonding zone at different joining times: (a) 45 min; (b) 60 min; (c) 75 min; (d) 100 min (Hadibeyk et al., 2018).

highest value of shear strength was achieved after homogenization heat treatment (34% stronger than 100 min bond) (Hadibeyk et al., 2018).

*MBF-20 foil interlayer, IN718 to IN600:*Jamaloei et al. (2017) investigated the dissimilar TLP bonding between IN718 and IN600 using a BNi-2 interlayer (MBF-20). Bonding was performed in a vacuum furnace at 1050 and 1100 °C, with bonding times varying from 5 to 45 min. Homogenization treatments were also performed, at 1180 °C for 180 min. The microstructure of the joint region was composed of three areas: the isothermal solidification zone (ISZ), athermally solidification zone (ASZ), and the diffusion affected zone (DAZ). Intermetallic compounds were found in the DAZ, and these were removed with the PBHT, it was found that increasing the bonding time and temperature lead to an increase in width of the DAZ. Hardness peaked in the DAZ, due to the presence of intermetallics. Boride compounds formed in the ASZ increased hardness also. Hardness in the ISZ was roughly equivalent to the base IN600 alloy. Due to the grain growth present during bonding, hardness reduced from the IN718 side to the IN600 side; this can also be attributed to the diffusion of strengthening elements of γ solid solution from IN718 to the joint area. Grain size in the parent material increased with the homogenization treatment from 12 to 10 μm for IN718 and IN600 respectively, to 115 and 220 μm. Bond shear strength increased with bonding time, and achieved a maximum after homogenization treatment (568 MPa). Complete isothermal solidification was obtained for the bonded specimen at 1050 °C and 1100 °C for 45 min and 30 min respectively. Fractography evaluation showed that the intermetallics at the bond center were the main reason for the propagation and growth of cracks (Jamaloei et al., 2017).

Foil interlayer, DD98 SX to K465: A microstructural study of TLP bonded single crystal DD98 and polycrystalline K465 nickel superalloys was completed by Liu et al. (2011). A 40–60 μm thick Ni-12Cr-3B interlayer was utilised for bonding. A vacuum furnace was used and the bonding conditions were 1190 °C for 2 h. Isothermal solidification of the liquid interlayer was incomplete after bonding at 1190 °C for 2 h, and many compounds formed from the remaining liquid interlayer upon cooling. Four kinds of phases formed: γ script like phase in the bond region, a dendritic phase which traverses the bonding zone, regular γ phase, and a blocky phase at the edge of the isothermally solidified region from the DD98 side. The script-like phase rich in Cr was CrB boride with a tetragonal structure. The dendritic phase that was enriched in Ni was $M_{23}B_6$ with an FCC crystal structure. The blocky phase was rich in Ti, Ta and Nb, and was identified to be MC carbide. Lots of Cr and W-rich blocky carbides with complex FCC structure are found in the diffusion zone on the K465 side. Borides were not present here. Blocky and platelet borides appeared in the diffusion zone on the DD98 side (Liu et al., 2011).

Composite sheet interlayer, TiAl to Ni-based superalloy: Dissimilar joining of TiAl alloy (4Ti-8Al-2Cr-2Nb) to Ni-based superalloy by laser welding using a V/Cu composite interlayer was investigated by Cai et al. (2019). The composition, microstructure and mechanical properties of the laser-welded joints were evaluated. The design of the composite interlayer is of great importance in dissimilar welding, and quite a complex interlayer was necessary in this study. After careful consideration and analysis, a two-sided V/Cu composite intelayer was chosen due to its diffusion characteristics and the inability to form hard intermetallics during the welding process. The V/Cu composite interlayer was kept in contact between the faying alloys in a self-constructed fixture. Single pass welding melted the composite interlayer and small amounts of the base metals to complete the weld. A pulse current of 85A/95A, plse duration 10 ms, pulse frequency 6 Hz, laser beam diameter 0.1 mm and welding speed of 180 mm/min were selected for welding parameters. Laser welding of TiAl alloy to NI-based superalloy has high crack sensitiviy, thus poor weldability. This is due to the formation of brittle intermetallic compounds with large differences in linear expansion coefficients. The formation of these compounds was greatly reduced when using the V/Cu interlayer. The resulting weld consisted mainly of V solid solution, Cu solid solution, less amount of $AlCu_2Ti$, and trace amounts of TiAl and NiAl phase. The composite interlayer improved the joint strength significantly, removing the brittle fracture behavior and allowing an average tensile strength of 230 MPa at room temperature and 145 MPa at 873 K, respectively. Welds fractured at the base metal at both high temperature and room temperature, Fig. 9 shows the surface morphology of the fractured joints (Cai et al., 2019).

*Foil interlayer, DD98 SX to M963:*Liu et al. (2010) conducted a study on the bonding behavior of nickel base single crystal (DD98) to poly-

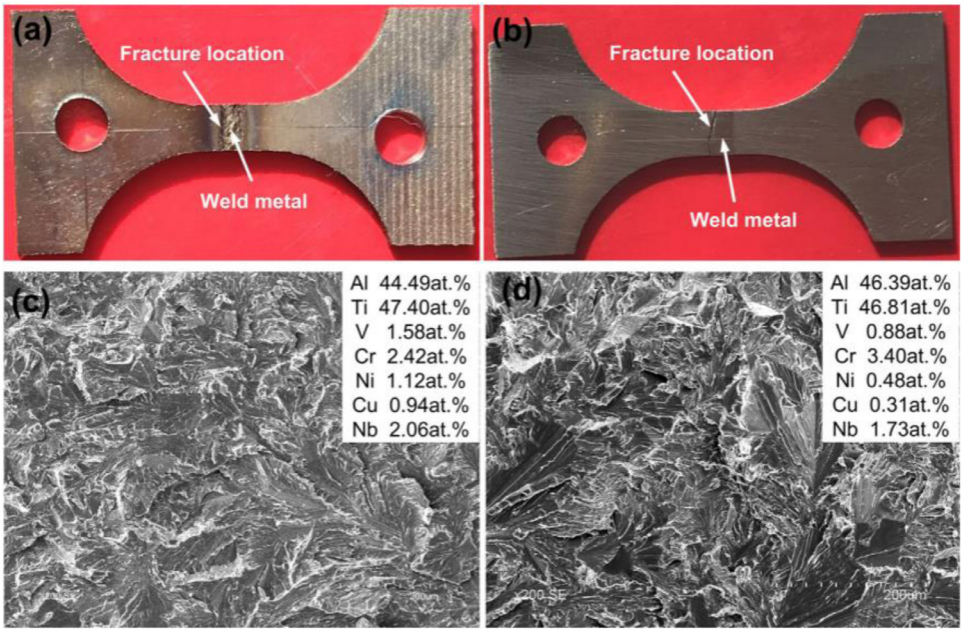

Fig. 9. Morphology of the fractured surfaces of the laser-welded join (a), (c) at room temperature and (b), (d) at 564 °C (Cai et al., 2019).

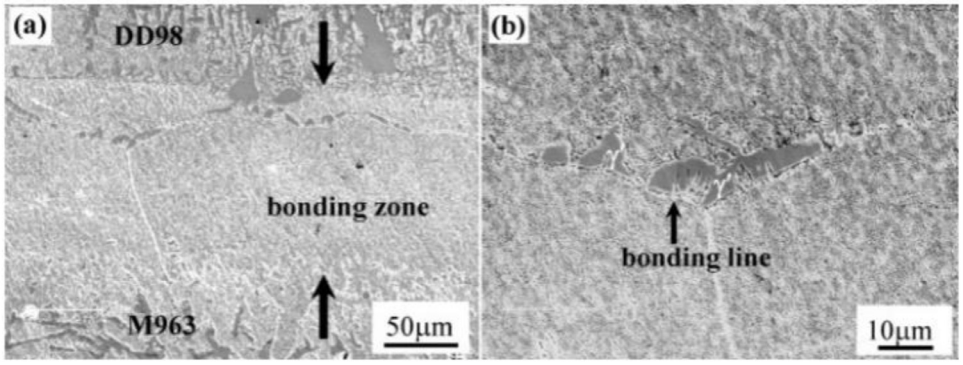

Fig. 10. SEM images of (a) the bonding zone, (b) the bonding line. The bond asymmetry can be seen here (Liu et al., 2010).

crystal (M963) superalloys by TLP method. The interlayer foil used was Ni-15Cr-3B amorphous alloy with thickness 40–60 μm. Bonding was performed in a vacuum furnace with a bonding pressure of 2.7 MPa, temperature of 1190 °C for various holding times. After 1190 °C for 4 h, the isothermal solidification process is over, and no trace of eutectic and carbides are found in the seam. Because of the difference in the diffusion coefficient of MPD, the isothermal solidifcation rate of polycrystal M963 was higher, this resulted in dissymety of bonding line during joining M963 and DD98, Fig. 10 (Liu et al., 2010).

*Foil interlayer, IN718 to 316 L Stainless Steel***:** As part of a fission surface power system technology from NASA, Locci et al. (2009) investigated the dissimilar bonding between IN718 and 316 L stainless steel via diffusion bonding and brazing. The microstructures and mechanical properties of both joints were analysed. Two classes of commercial brazing materials were evaluated, Nioro and AMDRY 109. Hot press diffusion bonding trials showed that bonding occurred with and without a pure nickel interlayer. Porosity was eliminated by higher bonding pressures. An aging heat treatment was required to restore most of IN718's strength after a typical Nioro brazing cycle. The stainless steel alloy, not affected from secondary phase precipitation or dissolution, maintained its ultimate tensile strength after a typical Nioro brazing cycle. It was concluded that Nioro is the leading braze candidate to join the two dissimilar metals for the HX application (Locci et al., 2009).

Foil interlayer, Ti_3Al to Ni superalloy: Laser joining of Ti_3Al-based alloy to Ni-based superalloy using a pure titanium interlayer was investigated by Cai et al. (2018). A YAG pulse laser with pure argon gas blown on the front and back of the specimens during welding to prevent oxidation. Dissimilar bonding of these materials without an interlayer results in very brittle and fragile laser welds that have poor mechanical properties. It was found that using the 0.4 mm pure titanium interlayers turned a fractured invalid joint into an effective Ti_3Al/Ni-based superalloy joint without macrocracks. The joint still had increased hardness over the base materials due to the formation of intermetallics, whichh resulted in consistent crack initiation sites during tensile tests. The average tensile strength and elongation of the interlayer joints were 177 MPa and 0.4% respectively. The ultimate tensile strength was still very low compared with the two base metals (Cai et al., 2018).

Nano-sputtering, IN718 to γ-TiAl: The joining of Inconel 718 to gamma-TiAl based duplex alloy using thin film deposition of Ni/Al interlayers has been investigated by Ramos et al. (2008). Direct current magnetron sputtering was used to deposit 5 and 14 nm multilayer thin films onto IN718 and TiAl. Solid-state diffusion bonding was use to join the dissimilar alloys, and the bonds were performed under vacuum in a tensile machine equipped with a furnace. Samples were heated to 800 °C and held for 1 h under a 50 MPa pressure. The role of the thin film multilayer was primarily to increase reactivity between the alloys, thus improving diffusivity at the lower than standard bonding temperature of 800 °C. It was found that the thin films significantly improved diffusion, this was confirmed via EDS analysis. The 5 nm multilayers resulted in some porosity and cracks inside the thin film, while 14 nm multilayers

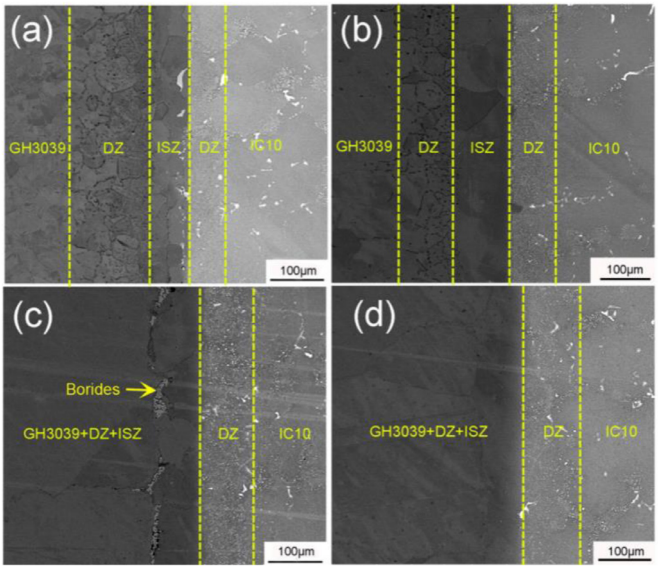

Fig. 11. SEM micrographs of the whole joints bonded at (a) 1050 °C for 2 h, (b) 1100 °C for 2 h, (c) 1150 °C for 2 h and (d) 1200 °C for 2 h. (Zhang et al., 2016).

allowed the joint quality to be improved and sound joining achieved along the central region of the bond. (Ramos et al., 2008)

Foil interlayer, IC10 SX to GH3039: Transient liquid phase bonding of IC10 single crystal to GH3039 alloy was carried out using a commercial BiNi2 interlayer by Zhang et al. (2016). TLP bonding was carried out in a vacuum furnace from 1050 to 1200 °C for 2 h. After bonding, the specimens were furnace cooled to room temperature in a vacuum. Typical microstructure of the TLP joint was composed of a diffusion zone (DZ), isothermal solidification zone (ISZ) and the base metal (BM). The DZ on the GH3039 side mainly consisted of Ni-Cr rick borides whereas the DZ on the IC10 side primarily consisted of γ' and MC type carbides. The ISZ was mainly γ solid solution. It was found that increasing the bonding temperature gradually decreased the precipitates until they vanished completely in the DZ on the GH3039 side. Precipitates on the IC10 side survived despite the variation in bonding temperatures. The microhardness of the joint became more uniform with increasing bonding temperature due to the suppresion of precipitates in the DZ on both sides. The room temperature tensile strength of the bonded joints could reach 90% of the base metal strength, though the joint bonded at 1150 °C had significantly worse strength due to the layers of borides in the bond region which acted as preferential crack initiation sites. Fig. 11 shows SEM micrographs of the bonded joints.

The formation mechanism of the TLP joint was summarized as follows: the interlayer metls first when reaching its melting point, the MPD element (boron atoms) then diffuse towards the base metal and the base metal adjacent to the liquid frontier dissovles subsequently. Due to microstructural differences of the base metals, a larger amount of the GH3039 alloy dissolves. After complete isothermal solidification, the final middle line moves towards the GH3039 side finally. The TLP bonding joint exhibits the characteristic of bonding asymmetry. (Zhang et al., 2016)

Powder mesh interlayer, Ni_3Al to NiAl-Hf SX: Gale and Wen (2001) investigated Ni_3Al based composite interlayers for wide gap dissimilar TLP bonding of NiAl-Hf single crystals to MM247 polycrystalline nickel superalloy. Bonds were performed at 1150 °C for up to 10 min. Due to the rapid isothermal solidification of the Ni_3Al-Cu interlayers, the bonding process could be complete after only 2 min at 1150 °C. This occurred due to the epitaxial growth of the bond line Ni_3Al particles dominating the isothermal solidification. Post bond heat treatments at 1000 °C removed the martensite and γ' deposits in the bond line, restoring the shear strength of the bond to that of the parent materials. Failure occurred in the bulk NiAl-Hf substrate, rather than at the bond line also (Gale and Wen, 2001).

Conclusions and recommendations

In joining of nickel alloys, the use of interlayer materials has consistently shown an improvement to bond integrity and strength (Stanners et al., 2020; Pouranvari et al., 2008; Zhai et al., 2014; Guo et al., 2017). Since compatibility of the mating materials is not an issue, the primary use case of interlayers over raw diffusion bonding is improving joint strength. Porosity is often reduced significantly with an interlayer, due to mechanisms such as 'powder collapse' which help fill the voids caused by surface asperities upon bonding (Stanners et al., 2020). Future development of this process should look at joining complex geometries and further improving bond strength.

In joining of dissimilar nickel alloys, a challenge that arises often is the difference in diffusivity of certain atoms in the two alloys. This can lead to bonding dissymmetry and hardness variation across the bondline (Liu et al., 2010; Zhang et al., 2016). This is typically overcome by modifying the interlayer composition, though changing the heating method to a more localized induction coil setup could allow for more controlled, focused heating that may allow for a temperature gradient across the two materials; meaning one could be at a slightly lower bonding temperature than the other. The formation of brittle intermetallics plagues almost every dissimilar joint, though bond performance is still improved over raw diffusion bonding via the use of an interlayer (Yang et al., 2019; Cai et al., 2018). Due to the added complexity of joining dissimilar nickel alloys, many studies did not include mechanical testing and rely only on microstructural analysis to judge the soundness of the bonds. This is understandable, as if compositional analysis shows a myriad of intermetallic-forming elements across the bond interface, one can assume the bond will not perform as well as its parent materials (Liu et al., 2011; Ramos et al., 2008). However, future studies should include mechanical testing to help understand the degree of strength gained over raw diffusion bonding or lost compared to the base alloys. The majority of dissimilar interlayer bonds utilize foil interlayers, other types of interlayer, such as powder-based, should be trialed more in future studies.

Post-bond heat treatments are common in interlayer joining of nickel-based alloys, proving to be necessary in many of the studies noted here, in both similar and dissimilar joining. Although not particularly an issue in laboratories, PBHTs would make on-site repairs of nickel-components much more challenging, due to the long treatment times. As this is one of the most promising factors of interlayer bonding, the hurdle that is PBHTs may need to be overcome for the process to achieve its potential. Clever manipulation of the interlayer material and bonding parameters can optimize the joining process to remove as many of the brittle intermetallics that form to disrupt the mechanical properties (Zhai et al., 2014; Zheng et al., 1993). Commercially available interlayers are being used in many investigations, showing an increase in demand for the benefit of interlayers for joining nickel alloys; these interlayers also act as great bases for one to build/ customize a more specific interlayer material.

Processes utilizing more specialized methods such as nano-sputtering interlayers have shown good joint quality (Ramos et al., 2008), but the development of more accessible and stable interlayers is perhaps more beneficial for the future of the process (Stanners et al., 2020; Li et al., 2003). Being able to prepare a bulk supply of interlayers that can be easily transported to a repair site would be an enticing development for the aerospace industry. Although using inert gas shielding has shown to have negative effects on some interlayer joints (Ekrami et al., 2007), it is significantly easier to implement for on-site repairs compared to vacuum bonding. It also works well with induction coil heating instead of furnace heating, as the level of control and the heating rate are much greater (Stanners et al., 2020). Decreasing the bonding time would improve the attractiveness of the interlayer process, as currently the time taken to

achieve sound bonding is a disadvantage when compared to traditional welding methods.

Author contributions

Conceptualization, W.R. and H.M.D.; software, W.R.; data curation, W.R.; writing-original draft preparation, W.R. and H.M.D.; writing-review and editing, W.R. and H.M.D.; supervision, H.M.D.; funding acquisition, H.M.D. All authors have read and agreed to the published version of the manuscript.

Funding

Rolls-Royce plc provided the funding for the current research and their contribution is gratefully recognized.

Declaration of Competing Interest

The authors declare no conflict of interest.

References

Akca, E., Gursel, A., 2015. The importance of interlayers in diffusion welding -a review. Period. Eng. Nat. Sci. 3S (3), 12–16. doi:10.21533/pen.v3i2.54.

Aluru, R., Gale, W.F., Chitti, S.V., Sofyan, N., Love, R.D., Fergus, J.W., 2008. Transient liquid phase bonding of dissimilar nickel base superalloys — wettability, microstructure and mechanical properties. Mater. Sci. Technol. 24 (5), 517–528. doi:10.1179/174328408X293478.

Aschenbruck, J., Adamczuk, R., Seume, J., 2014. Recent progress in turbine blade and compressor blisk regeneration. Procedia CIRP 22, 256–262.

Cai, X., Sun, D., Li, H, et al., 2018. Laser joining of Ti_3Al-based alloy to Ni-based superalloy using a titanium interlayer. Int. J. Precis. Eng. Manuf. 19, 1163–1169. doi:10.1007/s12541-018-0137-5.

Cai, X., Sun, D., Li, H., Meng, C., Wang, L., Shen, C., 2019. Dissimilar joining of TiAl alloy and Ni-based superalloy by laser welding technology using V/Cu composite interlayer. Opt. Laser Technol. 111, 205–213. doi:10.1016/j.optlastec.2018.09.053, ISSN 0030-3992.

Chandrappa, K., Kumar, A., Kumar, S., 2018. Diffusion bonding of a titanium alloy to a stainless steel with an aluminium alloy interlayer. IOP conference series. Mater. Sci. Eng. 402, 012124. doi:10.1088/1757-899X/402/1/012124.

Davies, P., Johal, A., Davies, H., Marchisio, S., 2019. Powder interlayer bonding of titanium alloys: Ti-6Al-2Sn-4Zr-6Mo and Ti-6Al-4V. Int. J. Adv. Manuf. Technol. 103, 441–452. doi:10.1007/s00170-019-03445-3.

Dunkerton, S., 2001. Joining Materials. TWI Ltd [Online]. Available: http://www.ansatt.hig.no/henningj/materialteknologi/Lettvektdesign/joining%20methods/joining-diffusion%20bonding.htm .

Ekrami, A., Moeinifar, S., Kokabi, A.H., 2007. Effect of transient liquid phase diffusion bonding on microstructure and properties of a nickel base superalloy Rene 80. Mater. Sci. Eng. A 456 (1–2), 93–98. doi:10.1016/j.msea.2006.12.044.

Gale, W.F., Wen, X., 2001. Ni_3Al based composite interlayers for wide gap transient liquid phase bonding of NiAl–Hf single crystals to a nickel base superalloy. Mater. Sci. Technol. 17 (4), 459–464. doi:10.1179/026708301101510050.

Guo, W., Wang, H., Jia, Q., Peng, P., Zhu, Y., 2017. Transient liquid phase bonding of nickel-base single crystal alloy with a novel Ni-Cr-Co-Mo-W-Ta-Re-B amorphous interlayer. High Temp. Mater. Process. 36 (7). doi:10.1515/htmp-2015-0243.

Hadibeyk, S., Beidokhti, B., Sajjadi, S.A., 2018. Effect of bonding time and homogenization heat treatment on the microstructure and mechanical properties of the transient liquid phase bonded dissimilar GTD-111/FSX-414 TLP superalloys. J. Alloy. Compd. 731, 929–935. doi:10.1016/j.jallcom.2017.10.105, ISSN 0925-8388.

Hunziker, O., Dye, D., Roberts, S.M., Reed, R.C., 1999. A Coupled approach for the prediction of solidification cracking during the welding of superalloys.. Conf on Numerical Analysis of Weldability. Graz-Seggau, Austria.

Jamaloei, A.D., Khorram, A., Jafari, A., 2017. Characterization of microstructure and mechanical properties of dissimilar TLP bonding between IN718/IN600 with BNi-2 interlayer. J. Manuf. Process. 29, 447–457. doi:10.1016/j.jmapro.2017.09.010, ISSN 1526-6125.

Khakian, M., Nategh, S., Mirdamadi, S., 2015. Effect of bonding time on the microstructure and isothermal solidification completion during transient liquid phase bonding of dissimilar nickel-based superalloys IN738LC and Nimonic 75. J. Alloy. Compd. 653, 386–394. doi:10.1016/j.jallcom.2015.09.044, ISSN 0925-8388.

Li, W., Jin, T., Sun, X.F., Guo, Y., Guan, H.R., Hu, Z.Q., 2003. Study of Ni–Cr–Co–W–Mo–B interlayer alloy and its bonding behavior for a Ni-base single crystal superalloy. Scr. Mater. 48 (9), 1283–1288. doi:10.1016/S1359-6462(03)00045-9, IssueISSN 1359-6462.

Liu, J., Cao, J., Lin, X., Song, X., Feng, J., 2013. Microstructure and mechanical properties of diffusion bonded single crystal to polycrystalline Ni-based superalloys joint. Mater. Des. 49, 622–626. doi:10.1016/j.matdes.2013.02.022.

Liu, J.-.D., Jin, T., Zhao, N.-.R., Wang, Z.-.H., Sun, X.-.F., Guan, H.-.R., Hu, Z.-.Q., 2010. Bonding behavior of nickel base single crystal to polycrystal superalloys by transient liquid phase method. Sci. Technol. Weld. Join. 15 (3), 194–198. doi:10.1179/136217109X12518083193513.

Liu, J.-D., Jin, T., Zhao, N.-R., Wang, Z.-H., Sun, X.-F., Guan, H.-R., et al., 2011. Microstructural study of transient liquid phase bonded DD98 and K465 superalloys at high temperature. Mater. Charact. 62 (5), 545–553. doi:10.1016/j.matchar.2011.03.012, IssueISSN 1044-5803.

Liu, M., Sheng, G., He, H., Jiao, Y., 2017. Microstructural evolution and mechanical properties of TLP bonded joints of Mar-M247 superalloys with Ni-Cr-Co-W-Ta-B interlayer. J. Mater. Process. Technol. 246, 245–251. doi:10.1016/j.jmatprotec.2017.03.021.

Locci, I.E., Bowman, C.L., Gabbs, T.P., 2009. Development of high temperature dissimilar joint technology for fission surface power systems. In: *Proceedings of the 4th International Brazing and Soldering Conference* (IBSC).

Malekan, M.F., Mirsalehi, S.E., Saito, N., Nakashima, K., 2019. Effect of bonding temperature on the microstructure and mechanical properties of Hastelloy X superalloy joints bonded with a Ni–Cr–B–Si–Fe interlayer. J. Manuf. Process. 47, 129–140. doi:10.1016/j.jmapro.2019.09.030, ISSN 1526-6125.

Pouranvari, M., Ekrami, A., Kokabi, A.H., 2008. Microstructure development during transient liquid phase bonding of GTD-111 nickel-based superalloy. J. Alloy. Compd. 461 (1–2), 641–647. doi:10.1016/j.jallcom.2007.07.108.

Preuss, M., Withers, P.J., Baxter, G.J., 2006. A comparison of inertia friction welds in three nickel base superalloys. Mater. Sci. Eng. A 437 (1), 38–45. doi:10.1016/j.msea.2006.04.058, IssueISSN 0921-5093.

Ramos, A.S., Vieira, M.T., Simões, S., Viana, F., Vieira, M.F., 2008. Joining of superalloys to intermetallics using nanolayers. Adv. Mater. Res. 59, 225–229. doi:10.4028/www.scientific.net/amr.59.225.

Sekhar, N.C., Reed, R.C., 2002. Power beam welding of thick section nickel base superalloys. Sci. Technol. Weld. Join. 7 (2), 77–87. doi:10.1179/136217102225002628.

Stanners, O., John, S., Davies, H.M., Watkins, I., Marchisio, S., 2020. The effect of processing variables on powder interlayer bonding in nickel-based superalloys. Mater. Basel 13, 601. doi:10.3390/ma13030601, (2020).

Tarai, U.K., Robi, P., Pal, S., 2018. Development of a novel Ni-Fe-Cr-B-Si interlayer material for transient liquid phase bonding of inconel 718. IOP Conf. Ser. Mater. Sci. Eng. 346, 012048. doi:10.1088/1757-899X/346/1/012048.

Torun, O., Celikyurek, I., 2008. Diffusion bonding of nickel aluminide Ni75Al25 using a pure nickel interlayer. Intermetallics 16 (3), 406–409. doi:10.1016/j.intermet.2007.11.011, IssueISSN 0966-9795.

Tuah-Poku, I., Dollar, M., Massalski, T., 1988. A study of the transient liquid phase bonding process applied to a Ag/Cu/Ag sandwich joint. Metall. Trans. A Trans. A 19, 675–686.

Tuppen, S., Bache, M., Voice, W., 2006. Structural integrity of diffusion bonds in Ti–6Al–4V processed via low cost route. Mater. Sci. Technol. 22, 1423–1430. doi:10.1179/174328406X129922.

Wikstrom, N.P., Ojo, O.A., Chaturvedi, M.C., 2006. Influence of process parameters on microstructure of transient liquid phase bonded Inconel 738LC superalloy with Amdry DF-3 interlayer. Mater. Sci. Eng. A 417 (1–2), 299–306. doi:10.1016/j.msea.2005.10.056, IssuesISSN 0921-5093.

Xiong, J., Yuan, L., Zhu, Y., Zhang, H., Li, J., 2019. Diffusion bonding of nickel-based superalloy GH4099 with pure nickel interlayer. J. Mater. Sci. 54, 6552–6564. doi:10.1007/s10853-018-03274-x.

Yang, Z.W., Lian, J., Wang, J., Cai, X.Q., Wang, Y., Wang, D.P., … Liu, Y.C., 2019. Diffusion bonding of Ni3Al-based alloy using a Ni interlayer. J. Alloy. Compd., 153324 doi:10.1016/j.jallcom.2019.153324.

Zhai, Q., Xu, J., Lu, T, Xu, Y., 2014. Research on interlayer Alloys for transient liquid phase diffusion bonding of single crystal nickel base superalloy DD6. J. Mater. Sci. Chem. Eng. 2, 12–19. doi:10.4236/msce.2014.29002.

Zhang, L.X., Sun, Z., Xue, Q., Lei, M., Tian, X.Y., 2016. Transient liquid phase bonding of IC10 single crystal with GH3039 superalloy using BNi2 interlayer: microstructure and mechanical properties. Mater. Des. 90, 949–957. doi:10.1016/j.matdes.2015.11.041.

Zheng, Y., Zhao, L., Tangri, K., 1993. Microstructure of Ni-10Co-8Cr-4W-13Zr alloy and its bonding behavior for single-crystal nickel-base superalloy. J. Mater. Sci. 28, 823–829. doi:10.1007/BF01151264.